Isı Bilimi ve Tekniği Dergisi, 33, 1, 01-09, 2013
J. of Thermal Science and Technology

ISSN 1300-3615

EFFECTS OF GEOMETRY AND NUMBER OF HOLLOW ON THE PERFORMANCE OF RECTANGULAR FINS IN MICROCHANNEL HEAT SINKS

H. J. TONY TAN*, M.Z. ABDULLAH and M. ABDUL MUJEEBU
Universiti Sains Malaysia, School of Mechanical Engineering, Engineering Campus, 14300 Nibong Tebal, Penang, Malaysia, *tonytan89@hotmail.com, Phone: +60164229648

(Geliş Tarihi : 31.03.2011 Kabul Tarihi:24.06.2011)

Abstract: This article presents the study on the effects of number and geometry of hollow on the heat transfer through rectangular fins attached to microchannel heat sinks. 3-dimensional models of microchannel heat sink with various hollow configurations inside the fins are developed for the analysis. The physical models are built and meshed in GAMBIT 2.3.26, and simulated by using the FVM-based CFD code, FLUENT 6.3.26. Three hollow geometries such as circular, rectangular and trapezoidal are introduced inside the rectangular fins, and simulations are performed with single hollow followed by double hollow. The results are obtained in terms of velocity profile, pressure drop, temperature distributions on the heat sink structure and base, and the total thermal resistance. It is observed that, the 'hollowed' fins could yield better hydrodynamic and thermal performances compared to the solid fins. Moreover, increase of number of hollows shows further improvement in performance, while the change in hollow geometry has negligible influence. The present model is validated with the theoretical correlations of previous workers and found in good agreement.
Keywords: Microchannel heat sink; Hollow profile fin; Heat transfer.

BOŞLUK GEOMETRİSİ VE SAYININ MİKROKANAL ISI KUYULARINDAKİ DİKDÖRTGEN KANATÇIKLARI ÜZERİNDEKİ PERFORMANSI

Özet: Bu makale mikrokanallardaki ısı kuyularına bağlı olan dikdörtgen kanatçıkların sayısının ve boşluk geometrisinin ısı transferine etkisini sunmaktadır. Analiz için değişik geometride boşluğa sahip mikrokanal ısı kuyularının 3-boyutlu modelleri geliştirilmiştir. Fiziksel modeller GAMBIT 2.3.26 programı ile çizilmiş ve ağ yapısı oluşturulmuş, FLUENT 6.3.26, sonlu hacimler yöntemi temelli HAD yazılımı ile simülasyonları yapılmıştır. Dikdörtgen kanatçıkların içerisinde dairesel, dikdörtgen ve yamuk kesitli boşluklar oluşturulmuş ve simülasyonlar önce tek boşluklu sonra çift boşluklu olarak gerçekleştirilmiştir. Sonuçlar, hız profili, basınç düşümü, ısı kaynağında ve tabanında sıcaklık dağılımları ve toplam ısıl direnç olarak elde edilmiştir. "İçi boşaltılmış" kanatçıkların katı kanatçıklara göre daha iyi hidrodinamik ve ısıl performansları olduğu görülmüştür. Ayrıca, boşluk geometrisindeki değişimin performans üzerinde ihmal edilebilir etkisi varken, boşluk sayısının artması performansı iyileştirmektedir. Bu model, daha önceki çalışanların teorik korelasyonları ile doğrulanmış ve uyum içinde oldukları bulunmuştur.
Anahtar Kelimeler: Mikrokanal ısı kuyusu, Boşluk profilli kanatçık, Isı transferi.

INTRODUCTION

Rapid advancements in the electronic industry and eventual product miniaturization necessitated effective cooling systems to dissipate the high heat involved. As one of the viable options, micro and mini channel heat sinks were investigated by many researchers in the recent past, both experimentally and numerically. A brief review of the pertinent literature is presented as follows.

Experimental study on flow and heat transfer characteristics of deep rectangular microchannels under single-phase forced convection was reported by Harms *et al.* (1999). Similar work on laminar flow with hydraulic diameter from 106 μm to 307 μm was done by Park and Punch (2008). Qu and Mudawar (2002) performed experimental and numerical investigations on the pressure drop and heat transfer characteristics of single-phase micro-channel heat sink fabricated from oxygen-free copper and fitted with a polycarbonate plastic cover plate. The three-dimensional conjugate heat transfer model involving Navier–Stokes and energy equations was solved by simultaneously determining the temperature field in both the solid and liquid regions, and matched well with the experimental results. Garimella and Singal (2004) investigated the fluid flow and heat transfer in microchannels and identified the pumping requirements and suitable mechanisms for pumping in microchannels. In their extended study (Lee *et al.*, 2005), it was experimentally verified that the conventional correlations were adequate to predict the thermal behavior in single-phase flow through rectangular microchannels. Similar observation was also

reported by Agarwal *et al.* (2010) for the case of rectangular minichannels.

The hydrodynamic and thermal performances of microheat exchangers with square cross-section were analyzed experimentally by Garcia-Hernando *et al.* (2009). Sara and co-workers [Sara *et al.*, 2009; Barlay Ergu *et al.*, 2009] investigated the pressure drop and local mass transfer in a rectangular microchannel; the pressure measurements were carried out with distilled water as working fluid while mass transfer measurements with a chemical solution by using electrochemical limiting diffusion current technique. For a minichannel heat sink with single-phase laminar flow of water through small hydraulic diameters and a constant heat flux, Xie *et al.* (2009) numerically studied the effects of channel dimensions, channel wall thickness, bottom thickness and inlet velocity on the pressure drop, thermal resistance and the maximum allowable heat flux. A three-dimensional model of heat transfer and fluid flow in noncircular microchannel heat sinks was developed by Chen *et al.* (2009) who compared the thermal efficiencies of triangular, rectangular and trapezoidal microchannels, and the triangular one was found to be the best. Akyol and Bilen (2006) studied the forced convection on vertical hollow rectangular fin where the air was flowing around the fins in a channel. Besides this, Elshafei (2010) investigated the natural convection heat transfer from vertical perforated circular pin fins.

Though many researches were carried out on the horizontal solid fins, and few researches on the vertical hollow fins cases, the issue of forced convection heat transfer on various configurations of horizontal hollow inside the fin is yet to be addressed. So, in the present work, the effects of geometry and number of hollows on the thermal behavior of rectangular fins attached to micro channel heat sinks are studied. The term 'hollow' used in this article is defined as a free passage inside the fin, facilitating additional coolant flow. Three hollow geometries such as circular, rectangular and trapezoidal, are considered, and finite volume simulations are performed for all the geometries, with single and double hollow. The hydrodynamic and thermal performances in each case are compared with the base case (fins without hollow or 'solid fins').

METHODOLOGY

The Physical Model

The three dimensional (3D) model of the microchannel heat sink, of size 60 mm (length, L) × 24.8mm (width, W) × 2 mm (height, H), is shown in Fig. 1. It consists of 11 channels (M1 to M11) with the dimensions of 42mm (length) × 0.80mm (width) × 1.60mm (height) and 10 fins (H1 to H10), as indicated in Figure 2. Keeping the dimensions of the channels and the fins fixed, simulations are performed on various configurations, such as solid fin, and fins with single and double hollows of rectangular, circular and trapezoidal geometries, as illustrated in Figure 3 (cases A, B1, B2, C1, C2, D1 and D2).

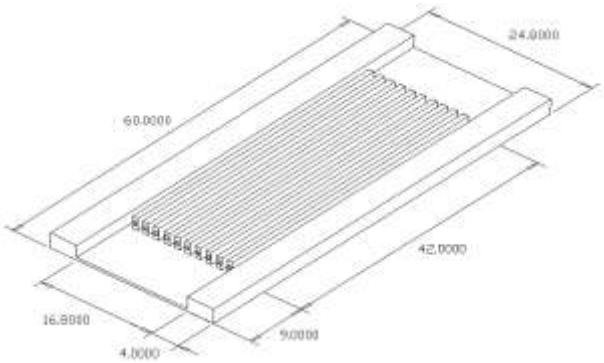

Figure 1. The microchannel heat sink model with dimensions (in mm).

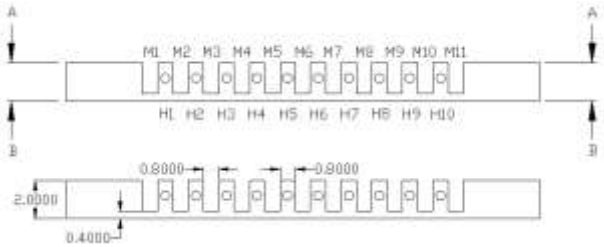

Figure 2. The cross sectional side view of the heat sink showing the channels (M1 to M11) and fins (H1 to H10), and the dimensions (in mm).

Computational Model

The fluid flow is assumed as steady state, single phase and laminar viscous. Other assumptions include, steady state heat transfer, constant material properties for fluid and heat sink, and surfaces exposed to ambient are adiabatic except the bottom which is communicated to the CPU chip. The governing equations are listed as follows.

Continuity equation:

$$\frac{\partial u}{\partial x}+\frac{\partial v}{\partial y}+\frac{\partial w}{\partial z}=0 \quad (1)$$

Navier – Stokes equation:

$$u\frac{\partial u}{\partial x}+v\frac{\partial u}{\partial y}+w\frac{\partial u}{\partial z}=-\frac{1}{\rho_f}\frac{\partial P}{\partial x}+\frac{\mu}{\rho_f}\left(\frac{\partial^2 u}{\partial x^2}+\frac{\partial^2 u}{\partial y^2}+\frac{\partial^2 u}{\partial z^2}\right) \quad (2a)$$

$$u\frac{\partial v}{\partial x}+v\frac{\partial v}{\partial y}+w\frac{\partial v}{\partial z}=-\frac{1}{\rho_f}\frac{\partial P}{\partial y}+\frac{\mu}{\rho_f}\left(\frac{\partial^2 v}{\partial x^2}+\frac{\partial^2 v}{\partial y^2}+\frac{\partial^2 v}{\partial z^2}\right) \quad (2b)$$

$$u\frac{\partial w}{\partial x}+v\frac{\partial w}{\partial y}+w\frac{\partial w}{\partial z}=-\frac{1}{\rho_f}\frac{\partial P}{\partial z}+\frac{\mu}{\rho_f}\left(\frac{\partial^2 w}{\partial x^2}+\frac{\partial^2 w}{\partial y^2}+\frac{\partial^2 w}{\partial z^2}\right) \quad (2c)$$

Energy equation- Fluid flow:

$$u\frac{\partial T}{\partial x}+v\frac{\partial T}{\partial y}+w\frac{\partial T}{\partial z}=\frac{k_f}{\rho_f c_{pf}}\left(\frac{\partial^2 T}{\partial x^2}+\frac{\partial^2 T}{\partial y^2}+\frac{\partial^2 T}{\partial z^2}\right) \quad (3)$$

It was reported (Koo and Kleinstreuer, 2004) that the viscous dissipation effect would be significant for flows in channels with hydraulic diameter less than 50 μm, and for fluids with low heat capacity and high viscosity. In the present study, as the hydraulic diameter is 1067μm, and the working fluid (water) has relatively high heat capacity and low viscosity, the viscous dissipation is neglected.

Case A : Solid fin

Single – hollow fin

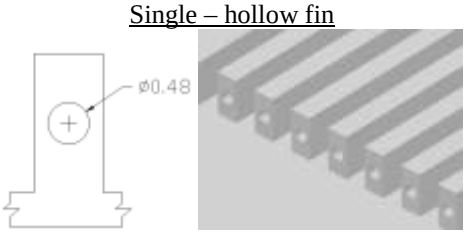

Case B1: One circular hollow

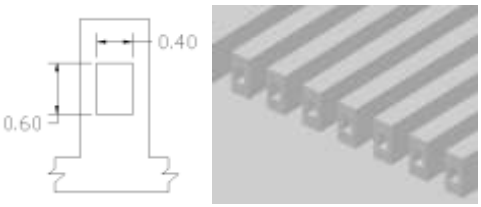

Case C1: One rectangular hollow

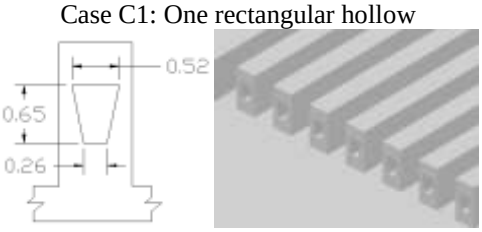

Case D1: One trapezoidal hollow

Double- hollow fin

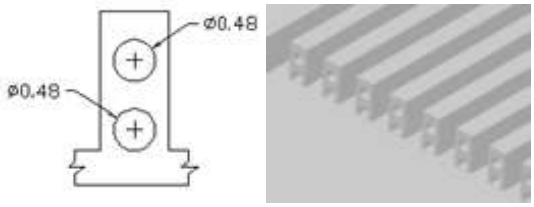

Case B2: Two circular hollows

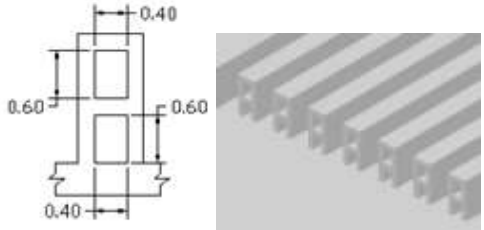

Case C2: Two rectangular hollows

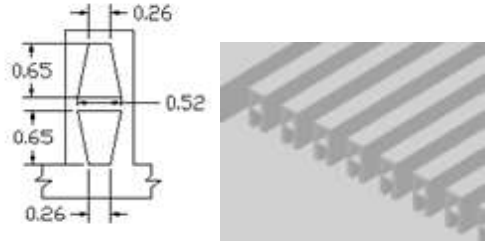

Case D2: Two trapezoidal hollows

Figure 3. Solid fin and fins with various hollow geometries.

Energy equation – Solid:

$$\frac{\partial^2 T}{\partial x^2} + \frac{\partial^2 T}{\partial y^2} + \frac{\partial^2 T}{\partial z^2} = 0 \quad (4)$$

The boundary conditions are:

At inlet of microchannel heat sink:

$u = u_{in}$; $T = T_{in}$ (5a)

Interface between solid and fluid:

$u = v = w = 0$ ms^{-1}; $T = T_s$;

$$-k_s \frac{\partial T_s}{\partial n} = -k_f \frac{\partial T}{\partial n} \quad (5b)$$

At the microchannel heat sink base:

$$q" = -k_s \frac{\partial T_s}{\partial n} \quad (5c)$$

At the outlet of the heat sink:

$P = P_{out}$;

$$\frac{\partial T}{\partial n} = 0 \quad (5d)$$

In equations (2a), (2b), (2c), (3), (5b) and (5c), the subscripts f and s refer to fluid and solid (heat sink structure), respectively.

The working fluid is water, and the heat sink material is aluminium; properties of these materials are summarized in Table 1. The fluid temperature at the heat sink inlet is 300K. The performance of microchannel heat sink is analyzed for volume flow rates from 0.9×10^{-5} m^{3}s^{-1} to 1.3×10^{-5} m^{3}s^{-1}. A heat flux of 200000 W/m^2 is assumed at the heat sink base.

Table1. Properties of water and aluminum (Holman, 1992).

Properties	Domain Substance	
	Water (at 300K)	Aluminum
Density (kg/m^3)	995.8	2707
Specific heat (J/kg.K)	4179	896
Conductivity (W/m.K)	0.614	204
Dynamic viscosity, μ (Ns/m^2)	0.00086	-

Meshing is performed with mix of two types of meshes such as hexahedral and wedge, according to the complexity of the locations. SIMPLE algorithm is selected to solve the governing equations. The pressure terms are discretized by Standard discretization, and momentum and energy equations are discretized by second order upwind scheme. The simulation took around 8 h in Intel (R) Xeon (R) CPU W3520 processor of 2.67 GHz, with RAM of 12.0 GB.

Grid Independency Test

In order to ensure grid independency, the velocity and temperature are observed for four sizes of grids, in each case. For case A, the mesh sizes were 5.70×10^5, 6.89×10^5, 9.65×10^5, and 11.66×10^5. Referring to Fig. 4 and Fig. 5, the velocity and temperature curves for various grid sizes show that the mesh sizes of 9.65×10^5, and 11.66×10^5 are almost close to each other, the difference being less than 1% only; hence, the mesh size

of 9.65 $\times 10^5$ is chosen for case A. Similar procedure is used for the other cases as well, as summarized in Table 2 which illustrates that the optimum mesh sizes for cases B1, B2, C1, C2, D1 and D2 are 16 08334, 2211755, 1534715, 1988441, 1518335 and 1898806 respectively. The notations Δab, Δbc and Δcd indicate the percentage variations in velocity/temperature obtained by two adjacent mesh sizes; for instance, Δab means the percentage deviation of velocity/temperature obtained by mesh size *b*, compared to *a*.

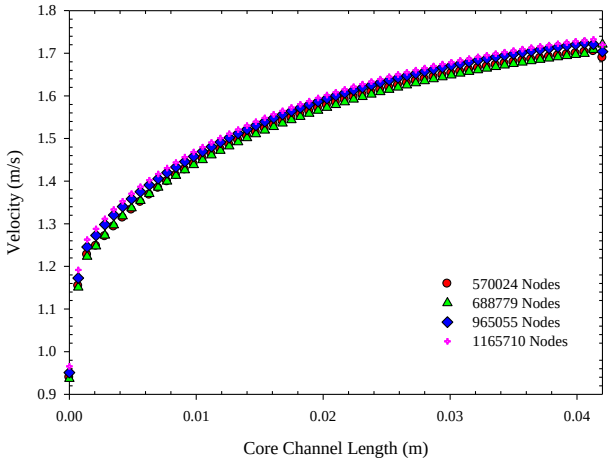

Figure 4. Velocity distribution along M6 in Case A for various grid sizes.

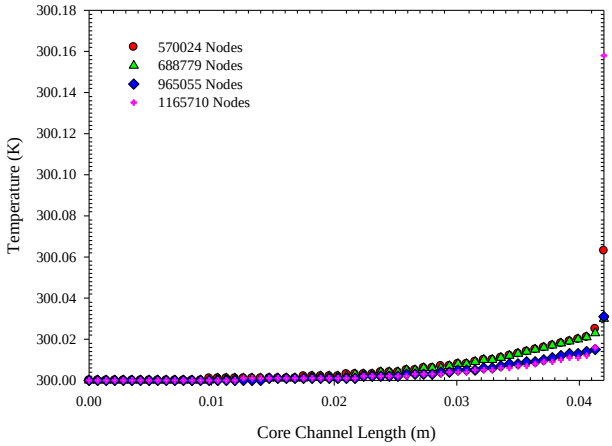

Figure 5. Temperature distribution along M6 in Case A for various grid sizes.

Table2. Summary of grid independence test for cases B1 to D2.

Cases →			B1	B2	C1	C2	D1	D2
Mesh size		*a*	834834	1107652	808444	1051414	800618	1007825
		b	1111019	1489397	1038765	1353807	1021839	1290289
		c	1608334	2211755	1534715	1988441	1518335	1898806
		d	1900444	2562378	1840566	2278458	1794793	2265172
% variation	Velocity	Δab	1.5186	0.9618	0.3924	0.5713	0.3778	0.7365
		Δbc	0.6790	0.8815	1.7270	0.7432	1.2716	0.7566
		Δcd	0.5649	0.2116	0.2762	0.1129	0.1101	0.3701
	Temp. 10^{-4}	Δab	1.0928	2.0764	0.49179	0.3825	0.05464	0.54643
		Δbc	6.2292	4.8086	6.9943	6.1746	6.6664	6.0654
		Δcd	1.8579	1.8032	0.81965	0.16393	3.1693	0.98358

Model Validation

By investigating fluid flow within the channels at *Re* between 789 and 1140, it is found that the hydrodynamic and thermal entry lengths (L_h and L_t respectively) are larger than the channel length. It shows that the fluid flow is hydrodynamically and thermally developing along the channel, as illustrated by the velocity and temperature profiles in Fig.4 and Fig.5 respectively. Therefore the theoretical correlations reported by Lei *et al.* (2006) (for hydrodynamically developing flow) and Kandlikar (2006) (for thermally developing flow), are used to validate the present model. Fig. 6 and Fig. 7 show the comparisons of predicted and theoretical results of pressure drop and average Nusselt number respectively; the average discrepancies are found to be 9.14% for pressure drop, and 7.85% for Nusselt number, which are acceptable.

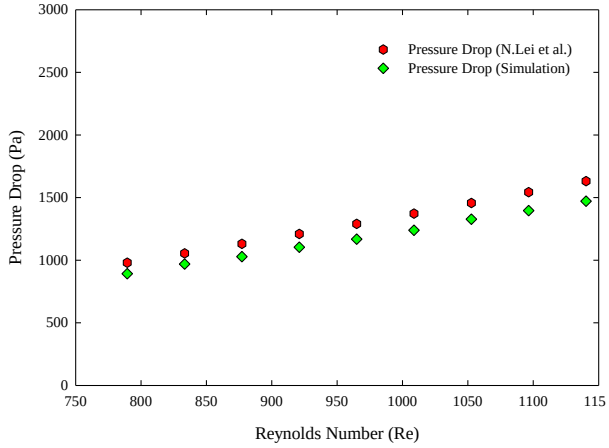

Figure 6. Average pressure drop for Case A- comparison between simulation and theoretical (Lei *et al.;* 2006) values.

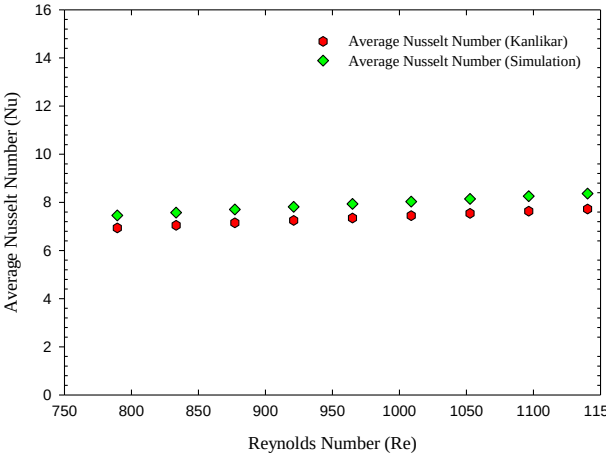

Figure 7. Average Nusselt number for Case A- comparison between simulation and theoretical (Kanlikar, 2006) values.

RESULTS AND DISCUSSION

Effects of Hollow and Its Geometry

Figure 8 shows the fluid velocity profiles within the channels and hollows for cases A, B1, C1 and D1, at volume flow rate of 1.3 $\times 10^{-5}$ m^3/s. As can be seen, velocity in the channel is higher than that in the hollow,

owing to the difference in flow resistances. Generally, the fluid flow distributions in the channels and the hollows are almost uniform, ensuring uniform heat dissipation across the microchannel heat sink structure as also emphasized by Senta and Agwu Nnanna (2007). It is interesting to note that, unlike the channels, the flow inside hollows is found to be fully developed, as indicated clearly by Fig.9. This is attributed to the fact that, the flow through small hydraulic diameters at low flow rates leads to low *Re* (laminar flow) (Kandlikar and Steinke., 2003) and becomes fully developed at a fairly earlier stage compared to the flow through the channels. The effect of hollow on the pressure drop across the heat sink is also analyzed, and the result is shown in Fig.10. It is observed that there is slight improvement in pressure drop by providing hollow, and the hollow geometry exhibited no significant influence.

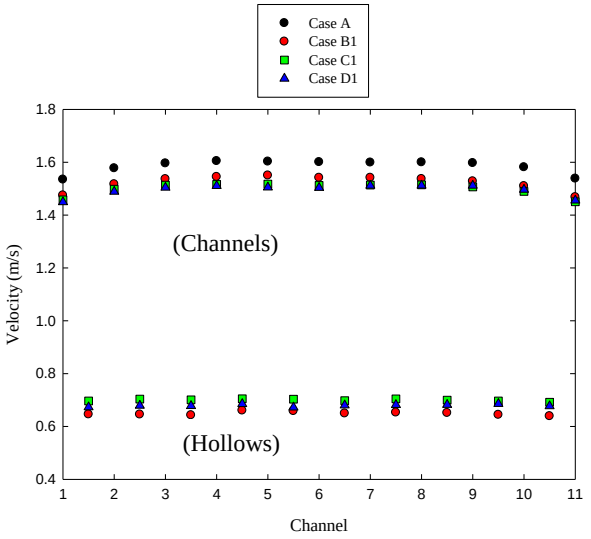

Figure 8. Comparison of velocity distributions of fluid flow across the channels and hollows among cases A, B1, C1 and D1.

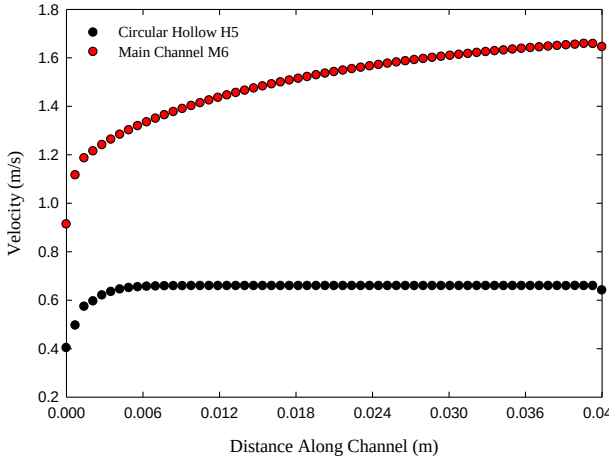

Figure 9. Comparison of velocity distributions between channel (M6) and hollow (H5).

Figure 11 shows the temperature contours near the top surface of the heat sink structure (section A-A in Fig. 2) with solid fins and single-hollow fins. In general, the initial section of the fins in each case is obviously showing low temperature, owing to the high convective heat transfer rate resulted by the large temperature gradient between the cool entering fluid and hot fin surface. This phenomenon was also reported by Chein and Chen (2009) and Chen *et al.* (2009). However, when hollow is introduced, the initial cool zone is significantly grown, presumably due to the enhanced heat transfer. Moreover, the presence of hollow could help cooling the hot spots at the heat sink edges, as well as the downstream regions of the fins, compared to the case A.

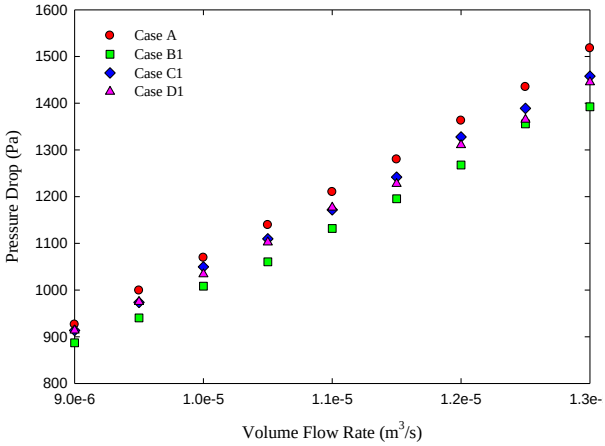

Figure 10. Comparison of pressure drop across the heat sink for cases with solid fin and single-hollow fins.

In order to further elucidate the benefit of hollowed fins, it is interesting to analyze the temperature of the heat sink base (section B-B in Fig. 2) which is directly exposed to the heat source. It is worth noting from Figs. 12 and 13 that, when hollow is introduced to the fins, the average base temperature is considerably reduced, which proves enhanced heat dissipation from the heat source. This is attributed to the additional exposed area of the fin for convection, causing the total thermal resistance to decrease. The total thermal resistance ($R_{th,total}$) is determined by Eq.(6) (Xie *et al.*, 2009) in which the terms on the right hand side represent thermal convective resistance, thermal capacity resistance and thermal conductivity resistance, respectively.

$$R_{th,total} = \frac{1}{\bar{h}A_{sf}} + \frac{1}{\dot{m}c_p} + \frac{1}{\left(\frac{k_S A_b}{H_b}\right)} \qquad (6)$$

where $\bar{h}$ is average convective heat transfer coefficient, H_b is heat sink base thickness, A_b is surafce area of the heated heat sink base, and A_{sf} is effective convective area of the fin.

As indicated in Fig. 14, $R_{th,total}$ decreases as the coolant volume flow rate increases. As expected, $R_{th,total}$ for Case A is the highest and significantly less for Cases B1, C1 and D1, in line with the low average heat sink base temperature as already seen in Fig. 13. Thus it is obvious that the presence of hollow can effectively improve the heat sink thermal performance. It is also observed that the hollow geometry has no remarkable influence on the thermal performance.

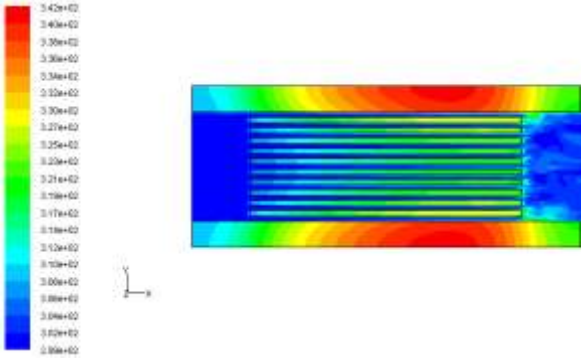

(a) Case A

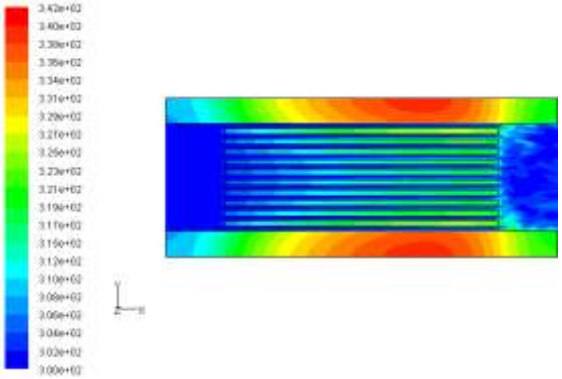

(b) Case B1

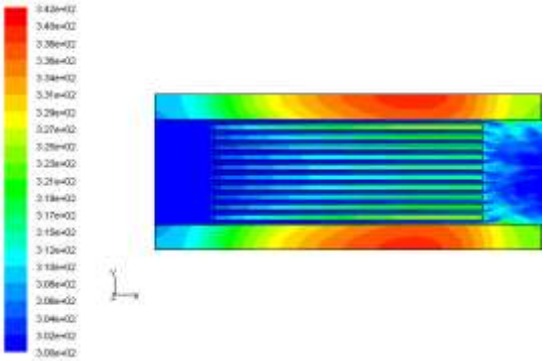

(c) Case C1

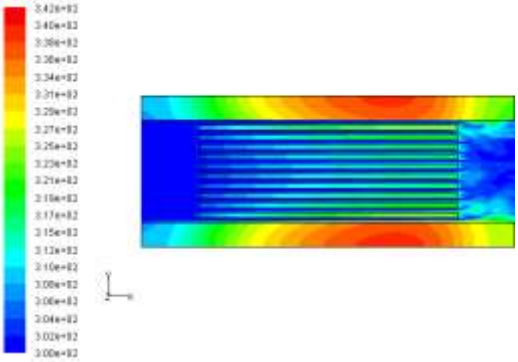

(d) Case D1

Figure 11. Temperature contour of heat sink structure with solid and single-hollow fins at volume flow rate of 1.3×10^{-5} m^3/s.

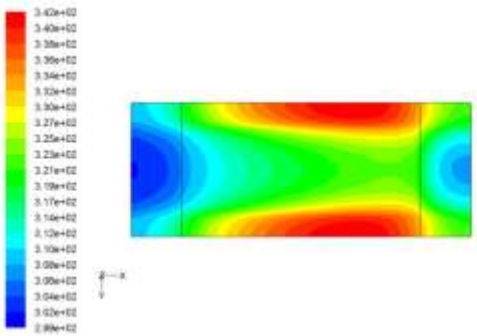

(a) Case A

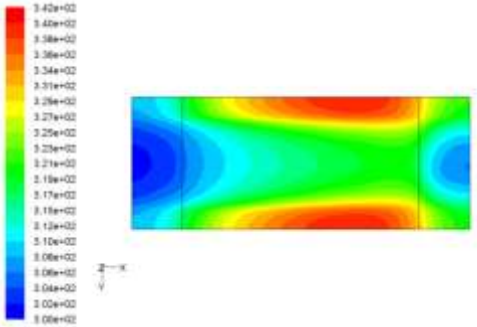

(b) Case B1

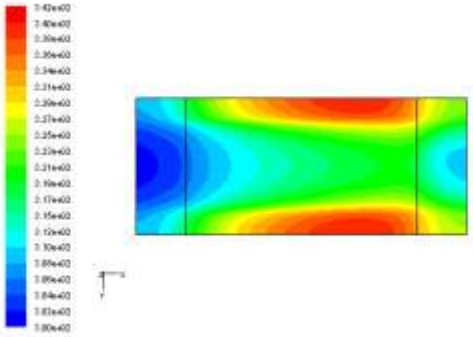

(c) Case C1

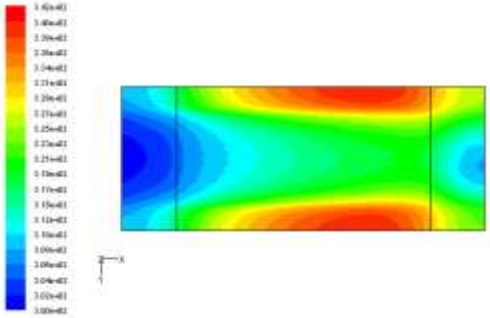

(d) Case D1

Figure 12. Temperature contour of heat sink base with solid and single-hollow fins at volume flow rate of 1.3×10^{-5} m^3/s.

Effect of Number of Hollows

Having convinced by the excellent impact of hollowed fins on the hydrodynamic and thermal performances of heat sinks, further simulations are performed to study the effect of number of hollows in a given fin. Referring to Fig. 15, it is worth noting that heat sink with the double- hollowed fins (cases B2, C2 and D2) shows slightly improved hydrodynamic performance (characterized by the decreased pressure drop) compared to the single-hollow case; this is attributed to the lower flow resistance. The average heat sink base temperature is further reduced with the increment of hollow, as observed in Fig. 16. This is elucidated further by the temperature contours shown in Fig. 17; the cool

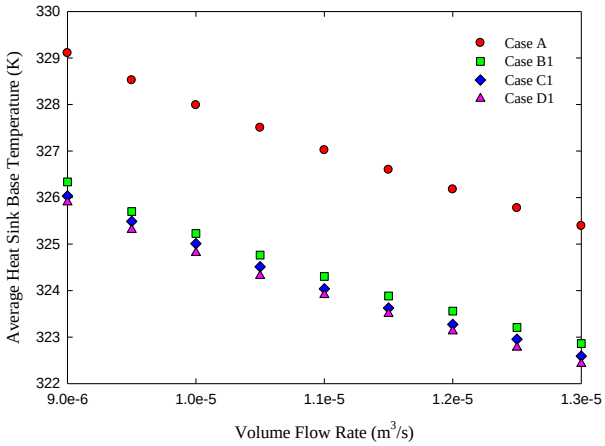

Figure 13. Average temperature of heat sink base with solid and single-hollow fins as function of volume flow rate.

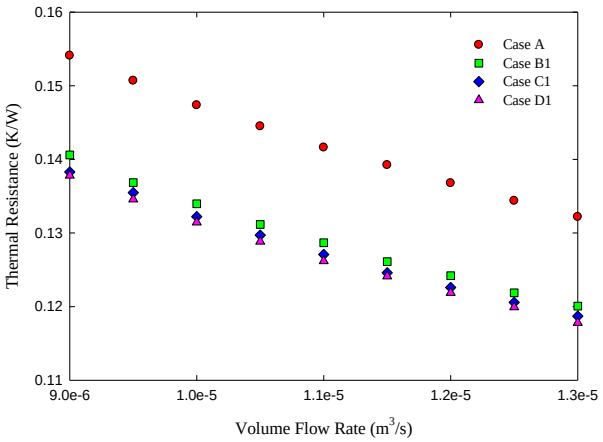

Figure 14. Comparison of total thermal resistance of heat sink with solid and single-hollow fins, as function of volume flow rate.

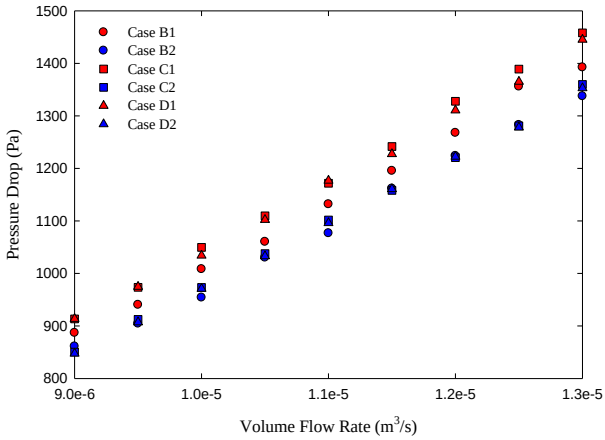

Figure 15. Pressure drop across the heat sink with single and double hollow fins as function of volume flow rate.

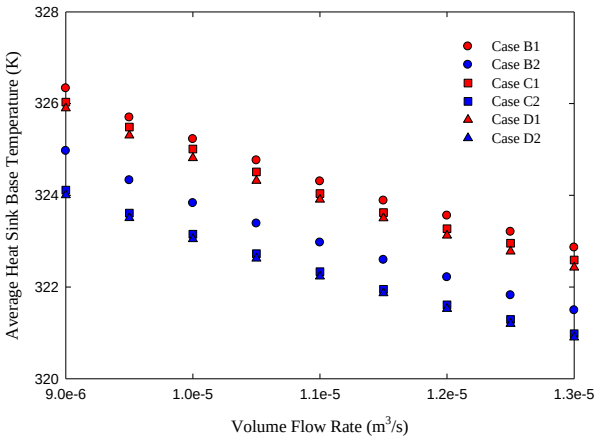

Figure 16. Average heat sink base temperature with single and double hollow fins as function of volume flow rate.

zone is spread wider in cases B2, C2 and D2, compared to the cases B1, C1 and D1.

Furthermore, as indicated by Fig.18, $R_{th,total}$ is reduced by increasing the number of hollow; reductions of 5.15%, 6.42%, and 6.21% are obtained for cases B2, C2 and D2 respectively, compared with B1, C1 and D1. It is also observed that, $R_{th,total}$ is not significantly affected by the hollow geometries. In general, by comparing $R_{th,total}$ of heat sink with double-hollowed fins with that of Case A, improvements of 13.84%, 16.04% and 16.34% are achieved for cases B2, C2 and D2 respectively. Thus it can be concluded that the introduction of hollows inside the fins could remarkably enhance the thermal performance of heat sinks.

CONCLUSION

Three-dimensional finite volume simulation is performed to study the effects of geometry and number of hollows inside rectangular fins, on the hydrodynamic and thermal performances of micro channel heat sink. The model is validated with the theoretical correlations of previous workers. Introduction of hollow inside the fins is proved to be promising for enhanced heat dissipation, weight reduction, and reduced coolant pumping power. Increasing the number of hollow decreases the overall thermal resistance of the heat sink, and the hollow geometry is found to be insignificant on the thermal performance. Being the first of its kind, this study needs further exploration in terms of experimental validation, and economic analysis and optimization to obtain trade-off between the feasibility of producing the hollow and the thermal benefit achieved through it.

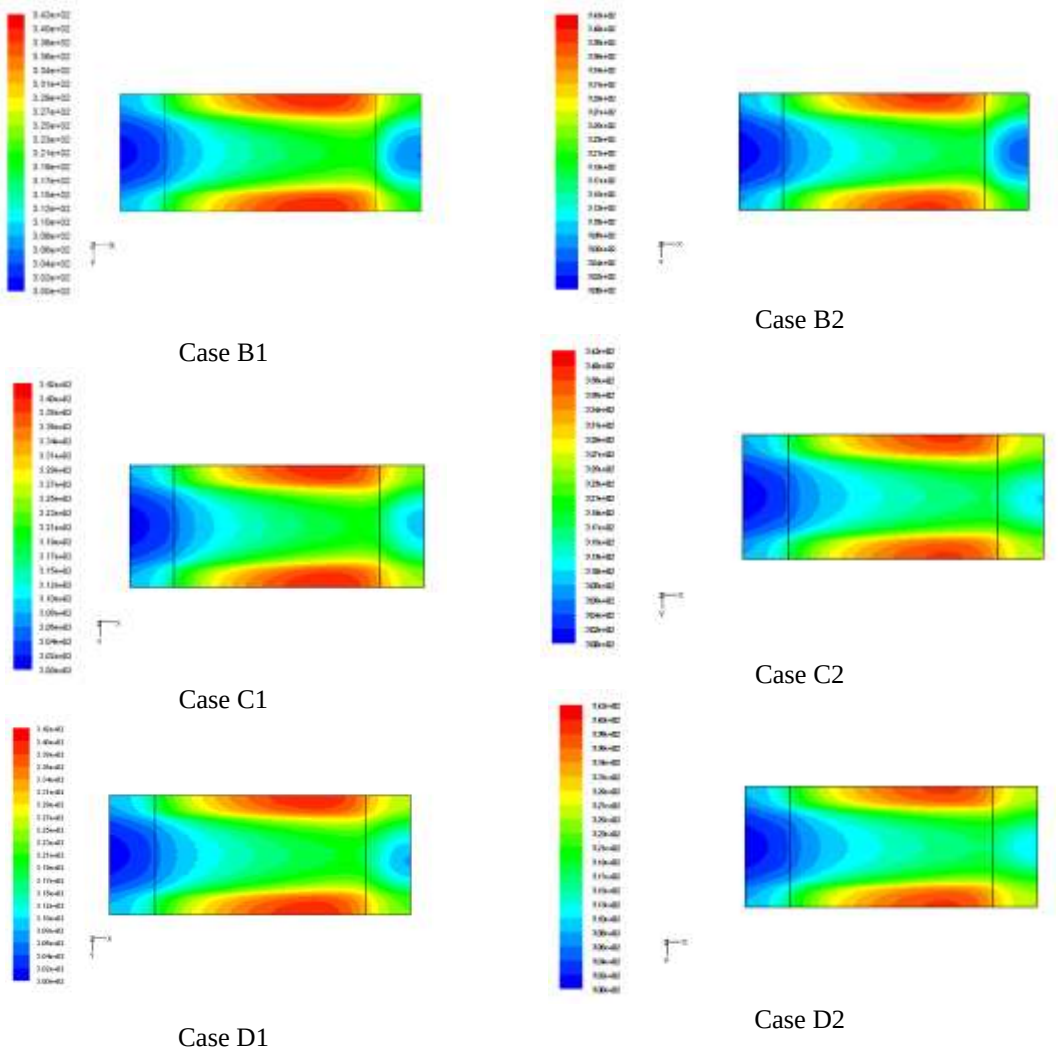

Figure 17. Temperature contours of heat sink base with single and double hollow fins at volume flow rate of 1.3×10^{-5} m^3/s.

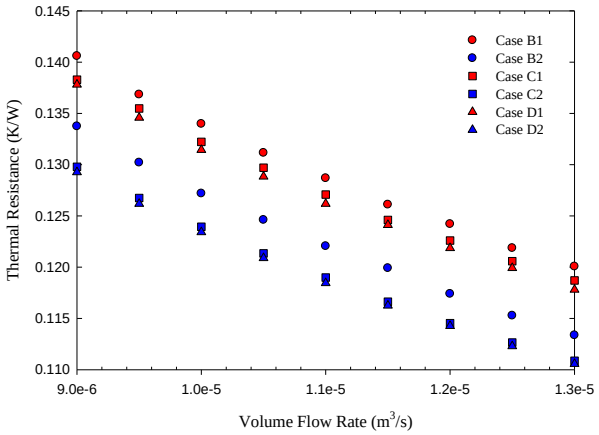

Figure 18. Total thermal resistance of heat sink with single and double hollow fins as function of volume flow rate.

REFERENCES

Agarwal G., Moharana M. K. and Khandekar S., 2010, Thermo-hydrodynamics of developing flow in a rectangular mini-channel array, *20th National and 9th International ISHMT – ASME Heat and Mass Transfer Conference 2010*; Research Publishing Services, ISBN: 978–981–08–3813–3,DOI: 10.3850/9789810838133_351.

Akyol U. and Bilen K., 2006, Heat transfer and thermal performance analysis of a surface with hollow rectangular fins, *Applied Thermal Engineering*, 26, 209 – 216.

Barlay Ergu O., Sara O. N., Yapici S. and Arzutug.M. E., 2009, Pressure drop and point mass transfer in a rectangular microchannel, *International Communications in Heat and Mass Transfer*, 36, 618 – 623.

Chein R. and Chen J., 2009, Numerical study of the inlet/outlet arrangement effect on microchannel heat sink performance, *Int. J.Thermal Sciences*, 48, 1627 – 1638.

Chen Y., Zhang C., Shi M. and Wu J., 2009, Three-dimensional numerical simulation of heat and fluid flow in noncircular microchannel heat sinks, *Int. Comm. in Heat and Mass Transfer*, 36, 917 – 920.

Elshafei E.A.M., 2010, Natural convection heat transfer from a heat sink with hollow/perforated circular pin fins, *Energy*, 1 – 8.

Garcia-Hernando N., Acosta-Iborra A., Ruiz-Rivas U. and Izquierdo M., 2009, Experimental investigation of fluid flow and heat transfer in a single-phase liquid flow micro-heat exchanger, *Int. J. Heat and Mass Transfer*, 52, 5433-5446.

Garimella S. V. and Singhal V., 2004, Single-phase flow and heat transport and pumping considerations in microchannel heat sinks, *Heat Trans. Eng.*, 25, 1, 15–25.

Harms T. M., Kazmierzak M. J. and Gerner F. M., 1999, Developing convective heat transfer in deep rectangular microchannels, *Int. J. Heat and Fluid Flow*, 20, 149-157.

Holman, J. P., 1992, Heat Transfer, 7th Edition, McGraw-Hill, Singapore.

Kanlikar S. G., 2006, Single-phase liquid flow in minichannels and microchannels, *Heat Transfer and Fluid Flow in Minichannels and Microchannels*, 87 – 136.

Kandlikar S. G. and Steinke M. E., 2003, Predicting heat transfer during flow boiling in minichannels and microchannels, *ASHRAE Transactions*, 109, 1, 1–9.

Koo J. and Kleinstreuer C., 2004, Viscous dissipation effects in microtubes and microchannels. *Int. Journal of Heat and Mass Transfer*, 47, 14-16, 3159-3169.

Qu W. and Mudawar I., 2002, Experimental and numerical study of pressure drop and heat transfer in a single-phase micro-channel heat sink, *International Journal of Heat and Mass Transfer*, 45, 2549 – 2565.

Lee P. S., Garimella S. V. and Liu D., 2005, Investigation of heat transfer in rectangular microchannels, *International Journal of Heat and Mass Transfer*, 48, 1688 – 1704.

Lei N., Skandakumaran P. and Ortega A., 2006, Experiments and modeling of multilayer copper minichannel heat sinks in single-phase flow, *0-7803-9524-7/06/© 2006 IEEE*, 9 – 18.

Park H. S. and Punch J., 2008, Friction factor and heat transfer in multiple microchannels with uniform flow distribution, *International Journal of Heat and Mass Transfer*, 51, 4535 – 4543.

Sara O .N., Barlay Ergu O., Arzutug M. E. and Yapici S., 2009, Experimental study of laminar forced convective mass transfer and pressure drop in microtubes, *International Journal of Thermal Sciences*, 1 – 7.

Senta M. and Agwu Nnanna A. G., 2007, Design of manifold for nanofluid flow in microchannels, *Proceedings of the ASME Int. Mechanical Engineering Congress and Exposition, No. IMECE2007-42720*, Seattle, Washington, 1-8.

Xie X. L., Liu Z. J., He Y. L. and Tao W. Q., 2009, Numerical study of laminar heat transfer and pressure drop characteristics in a water – cooled minichannel heat sink, *Applied Thermal Engineering*, 29, 64 – 74.